

Article

Mechanism and Control of Grout Propagation in Horizontal Holes in Fractured Rock

Zhaoxing Liu *, Shuning Dong, Hao Wang and Hongbo Shang

Xi'an Research Institute (Group) Co., Ltd., China Coal Technology and Engineering Group Corp.,
Xi'an 710054, China

* Correspondence: liuzhaoxing0417@foxmail.com

Abstract: It is important to control grout propagation and ensure the engineering effectiveness of the advanced regional grouting process in the Middle Ordovician limestone (MOL) aquifer. In our study, we found that the physical and mechanical properties of cement grout are affected mainly by the water–cement ratio, followed by water glass content and finally by hydro-chemical type. In a horizontal grouting hole inclined single fracture, the grout spread over time depended on the water–cement ratio, grouting pressure, width of fracture and angle between fracture and grouting hole and the rate of spread increased over time. However, when the grout propagation length was hundreds of meters or more, the length in the fracture above the grouting hole was greater than that in the fracture below. The sensitivity sequence of influencing factors of grout propagation length in an inclined fracture of a horizontal grouting hole was as follows, from large to small: width of fracture, fracture angle, water–cement ratio, grouting pressure.

Keywords: advanced regional grouting; grout propagation length; horizontal directional drilling; inclined single fracture; method of grout control; principle of cement grout



Citation: Liu, Z.; Dong, S.; Wang, H.; Shang, H. Mechanism and Control of Grout Propagation in Horizontal Holes in Fractured Rock. *Water* **2022**, *14*, 4062. <https://doi.org/10.3390/w14244062>

Academic Editors: Qiqing Wang and Shiliang Liu

Received: 26 October 2022

Accepted: 24 November 2022

Published: 12 December 2022

Publisher's Note: MDPI stays neutral with regard to jurisdictional claims in published maps and institutional affiliations.



Copyright: © 2022 by the authors. Licensee MDPI, Basel, Switzerland. This article is an open access article distributed under the terms and conditions of the Creative Commons Attribution (CC BY) license (<https://creativecommons.org/licenses/by/4.0/>).

1. Introduction

Surface-mined coal in the North China coalfields has been fully excavated because of the large-scale exploitation and use of coal resources. Most of its coal mines are being, or have been, classified as underground mining. Middle Ordovician limestone (MOL) aquifers, abundant under deeper coal seams, pose a serious water inrush threat to the safety of coal seam mining [1,2]. The permeability of the karst above MOL decreases due to weathering and filling, forming a relatively water-resistant stratum [3]. Fortunately, the thickness of the water-resisting strata beneath underground coal seams can be increased by sealing with grout or by reinforcement. In addition, because horizontal directional drilling technology has been improved, many mining areas (such as the Fengfeng, Xingtai and Feicheng mining areas) have adopted surface horizontal directional drilling to carry out advanced regional grouting on the top of the MOL [4–6]. This is called advanced regional grouting treatment of coal mine floors. The technology's effectively alleviates the threat of water inrush from the MOL aquifers. However, because the theory of grouting lags behind engineering practice, the selection of grouting parameters such as drilling spacing, grouting pressure and grout properties is still blind because it is merely based on experience. Consequently, current grouting processes lack effective control of grout propagation. Advanced regional grouting projects face impediments such as long construction periods, excessive grouting amounts and unreliable grouting effects. Therefore, it is necessary to study the mechanism and influence factors of grout propagation in horizontal grouting holes in fractured rock, in order to formulate a principle of grout ratio regulation and finally to achieve the goal of coal mine grouting propagation control.

The karst characteristics of MOL include dissolution fractures, karst caves, honeycomb karst pores, collapse columns and dissolution fractures. These are the most developed

features in the coalfield area of North China and form the main channels for groundwater storage and migration in that area [6]. Therefore, grout at the top of the MOL is propagated mainly in the rock fractures. Due to the complexity of the distribution of rock joints and fissures, determining the flow law of grout in rock fractures is complicated. Consequently, research on rock fracture grouting has focused mainly on the grout flow in a single fracture [7]. In addition, conventional grouting engineering has been based on vertical or oblique coal drilling, so models of rock fracture grouting have all been based on the intersection of vertical grouting holes and horizontal fractures [8–13] and the influence of gravity on cement grout itself has been ignored. However, grouting conditions on coal mine floors and drilling types for conventional grouting projects are different from those for advanced regional grouting treatment projects. Obviously, the grout propagation length in an advanced regional grout treatment project is greater than that of others and the influence of gravity on cement grout is more important [14,15]. Because karst fractures are the most common type in MOL, grout movement along the fractures can be predetermined. However, few studies have built a model of grout propagation based on inclined fractures of horizontal grouting holes or have devised a control technology for grout propagation in those types of fractures based on the properties of cement-based grout, the mechanism of grout propagation and the characteristics of a grouted rock mass.

In this study, we analyzed the regulation principle of grout according to the properties of the grout and its influencing factors. Considering those factors, we constructed a grout propagation model for an inclined single fracture in a horizontal grouting hole. By controlling variables, we also obtained the characteristics of grout propagation length under various influencing factors. Furthermore, we determined the influence of the sensitivity of each influencing factor on the grout propagation length based on a numerical simulation in an orthogonal experimental design. The research results provide practical guidance for using surface horizontal directional drilling for advanced regional grouting operations.

2. Characteristics of Macroscopic Vertical Permeability at the Top of a Middle Ordovician Limestone Layer

The total thickness of the MOL in China's Hanxing mining area is approximately 560 m; the layer is divided into three groups and eight sections [16]. The uppermost part of the three groups is the Fengfeng formation, the thickness of which is 133 to 188 m. That formation can be itself be divided into an eighth section, a seventh section and a sixth section from top to bottom. The thickness of the eighth section of the Fengfeng formation is 13 to 28 m, comprising mainly dolomitic brecciated limestone. The thickness of the seventh section is 70 to 110 m; it consists of thick, layered crystalline limestone. The limestone at the bottom of the seventh section contains breccia and has a strong water yield. Currently, the stratum that is the target of advanced regional grouting treatment projects is the eighth section of the Fengfeng formation. However, due to the thickness of that stratum, if the permeability of the layer under the target stratum is high, the grout easily propagates down during the grouting process and is wasted. Therefore, in typical coal mines in the Hanxing mining area, it is necessary to obtain the vertical permeability characteristics of the top stratum of the MOL based on an analysis of drilling data of the MOL top.

We can summarize the macroscopic vertical permeability characteristics of the top layer of the MOL of the Dongpang and Wutongzhuang mine in the Hanxing mining area by determining how much flushing fluid is consumed (Figure 1).

- (1) Dongpang mine: The flushing fluid leakages of a total of 88 boreholes were recorded. The end position of the No. 3 water source hole was in the upper Majiagou formation were is under the Fengfeng formation; the end positions of the others were in the Fengfeng formation. Among the 88 holes, only two holes did not leak and the other holes had various degrees of flushing fluid leakage. Within 10 m from the top of the MOL, the leakage of 90% of the boreholes was less than $1.0 \text{ m}^3\text{h}^{-1}$, which is categorized as slight leakage and the leakage of only one hole was greater than $10 \text{ m}^3\text{h}^{-1}$. In addition, according to the statistics for every 10 m at the top of the MOL

from 16 boreholes (Table 1), we found that the leakage within 40 m of the top of the MOL was minor and changed little, but the leakage of the flushing fluid increased markedly at deeper than 40 m. This indicates that the karst fracture rate in the upper 40 m of the MOL was relatively low, the water yield was weak and the water entered the strong aquifer part of the seventh section of the Fengfeng formation at a depth of 40 m.

- (2) Wutongzhuang mine: The leakages of 11 boreholes in the MOL strata of the Wutongzhuang mine were determined. Among them, the flushing fluid leakages of two boreholes decreased within 30 m of the top of the MOL; this is for 18% of the boreholes. The leakages were $5 \text{ m}^3\text{h}^{-1}$ and $40 \text{ m}^3\text{h}^{-1}$ when the lengths of the boreholes were 15 m and 24.5 m under the MOL, respectively, which indicates that the water yield property of the eighth section of the MOL was uneven but generally weak. The end positions of eight of the boreholes in the seventh section of the MOL, among which four boreholes had leakage of flushing fluid, accounted for 50% of the total boreholes. According to the analysis, there was a weathering crust at the top interface of the MOL and most of the cracks were filled with argillaceous components, so the water resistance was good. The MOL aquifer is zonal vertically. At 15 m below the top surface of the MOL, we found no leakage of flushing fluid from any boreholes; at 15 to 30 m, the water yield of the stratum was relatively weak and uneven; at more than 30 m, the water yield of the stratum was strong and uneven.

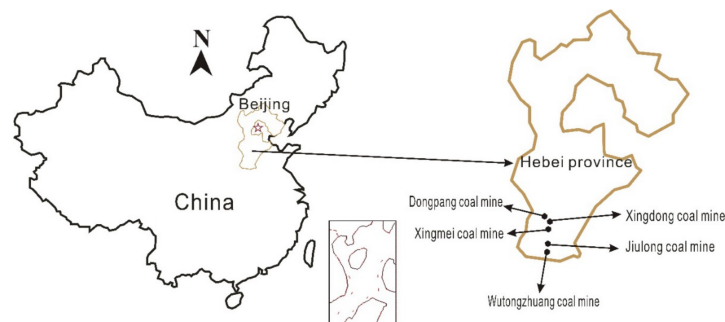


Figure 1. Distribution map of some of the coal mines in the study area.

Table 1. Number of boreholes with different depths and drilling flushing fluid consumption at the upper layer of the MOL and the average of drilling flushing fluid consumption at corresponding depths (Dongpang mine).

Leakage/ $\text{m}^3 \cdot \text{h}^{-1}$	Number of Boreholes at Different Depths				
	$\leq 10 \text{ m}$	10–20 m	20–30 m	30–40 m	$>40 \text{ m}$
≤ 0.1	5	5	7	7	3
0.1–1.0	9	9	7	6	6
1.0–10.0	2	2	2	3	5
>10.0	0	0	0	0	1
Average leakage	0.5	0.35	0.38	0.31	2.12

In summary, compared with the permeability and water abundance of the eighth and seventh sections of the Fengfeng formation, the seventh stage of water and permeability of the seventh sections of the Dongpang mine and the Wutongzhuang mine is better than the eighth. The vertical permeability of the Fengfeng formation can be obtained. In the process of grouting, the grouting material and the ratio of grout must be adjusted to prevent invalid diffusion of the grout.

3. Analysis of Cement Grout Performance and Its Influencing Factors

Because of environmental protection and construction technology, in an advanced regional grouting project, cement grout is mainly used. Therefore, the properties of ce-

ment grout and its influencing factors are very important for the development of grout technology and for control of grout propagation in projects. Although cement grout properties have been widely researched, the influence of the chemical characteristics of deep groundwater in grouted rock is rarely studied. Therefore, we analyzed the applicability and regulation principles of cement grout in advanced regional grouting projects based on experiments on the influence of various factors on cement grout and the characteristic of grout rock fractures.

3.1. Hydro-Chemical Characteristics of a Middle Ordovician Limestone Top

Li, Gao [17] used concentrated groundwater from an MOL aquifer to prepare loess–cement grout. Relative to loess–cement grout prepared with pure water, the initial setting duration was shortened, the strength at 28 days of age was greater and the impermeability was greater. Although the test was carried out to reduce the mine water discharge and floor grouting cost, it shows that Ordovician limestone groundwater has a significant effect on cement grout performance. Therefore, we regarded the influencing factor to be the chemical type of the MOL water and used that as the basis of studying the control factors of cement grout. For indoor hydro-chemical analysis tests, we sampled the groundwater at the top of the MOL aquifer in the Hanxing mining area and determined its chemical characteristics (Table 2).

Table 2. Hydro-chemical type and mineralization degree of an MOL aquifer in part of China’s Hanxing mining area.

Number	Mining	Borehole Number	Position	pH	Hydro-Chemical Type	Mineralization Degree/mg·L ⁻¹
a	Xingmei	D3	The eighth section of Fengfeng formation	8.17	HCO ₃ -Ca·Mg	336.07
b	Xingdong	T3	The seventh section of Fengfeng formation	8.85	SO ₄ -Ca·Mg	1690.37
c	Wutongzhuang	WO3	Fengfeng formation	7.09	Cl·SO ₄ -Ca·Na	5496.47
d	Jiulong	/	The seventh section of Fengfeng formation	7.75	Cl·SO ₄ -Ca·Na	4333.30

3.2. Test Scheme

In accordance with the L₁₆ (4⁵) orthogonal table, we carried out a performance test of cement grout with various contents of sodium silicate, various water–cement ratios and various groundwater hydro-chemical types of the top aquifer of the MOL in the Hanxing mining area (Tables 3 and 4).

Table 3. Test factors and levels of cement grout.

Level	Factors		
	Water–Cement Mass Ratio (A)	Content of Sodium Silicate/% (B)	Hydro-Chemical Type (Mining) (C)
1	0.6:1	0	a (Xingmei)
2	0.8:1	2	b (Xingdong)
3	1:1	5	c (Wutongzhuang)
4	2:1	8	d (Jiulong)

Table 4. Orthogonal test scheme for cement grout.

Test Number	Water–Cement Mass Ratio (A)	Content of Sodium Silicate/% (B)	Hydro-Chemical Type (Mining) (C)
1	0.6:1	0	a
2	0.6:1	2	b
3	0.6:1	5	c
4	0.6:1	8	d
5	0.8:1	0	b
6	0.8:1	2	a
7	0.8:1	5	d
8	0.8:1	8	c
9	1:1	0	c
10	1:1	2	d
11	1:1	5	a
12	1:1	8	b
13	2:1	0	d
14	2:1	2	c
15	2:1	5	b
16	2:1	8	a

3.3. Test Results

We determined the physical and mechanical property parameters of cement grout under a combination of various influencing factors (Table 5). The factors included viscosity, density, initial setting duration, final setting duration, stone rate and flexural and compressive strengths. A range analysis method was used to analyze the experimental results and we determined the range values of physical and mechanical parameters under the influence of various factors. The sensitivity of grout performance to various influencing factors can be judged by comparing various range values. The controlling factors of grout physical and mechanical properties can also be obtained (Table 6). Note that, in the ranking of the range results of various grout properties, all the properties were most sensitive to the water–cement ratio. The next most important factor was the influence of water glass content and the weakest was the Hydro-chemical type. Based on this, to control the properties of the grout in advanced regional grouting projects, the water–cement ratio should be adjusted first and then the water glass content.

Table 5. Orthogonal test results of cement grout.

Test Number	Influencing Factors			Physical and Mechanical Property Parameters										
	A	B	C	Viscosity/Pa.s	Density/g.cm ⁻³	Initial Setting Time/h	Final Setting Time/h	Stone Rate/%	Flexural Strength/MPa			Compressive Strength/MPa		
									3 d	7 d	28 d	3 d	7 d	28 d
1	0.6:1	0	a	0.30	1.64	10.08	13.00	95.40	2.47	2.75	4.88	6.09	8.32	18.74
2	0.6:1	2	b	0.58	1.57	8.92	11.33	97.10	2.50	3.13	4.71	6.79	10.68	16.36
3	0.6:1	5	c	0.88	1.56	6.08	8.42	98.40	2.42	3.34	4.86	6.37	10.34	16.29
4	0.6:1	8	d	1.24	1.51	4.33	6.58	99.20	1.69	2.73	3.50	4.17	9.12	14.98
5	0.8:1	0	b	0.16	1.45	11.33	15.10	84.65	1.77	2.37	4.43	3.65	6.22	18.32
6	0.8:1	2	a	0.22	1.42	9.50	11.83	90.75	1.25	1.73	3.52	3.33	5.93	11.66
7	0.8:1	5	d	0.67	1.41	7.25	10.08	93.05	1.14	1.54	2.75	3.00	4.68	9.29
8	0.8:1	8	c	0.79	1.39	5.17	7.67	96.50	1.13	1.54	2.57	2.93	4.42	8.43
9	1:1	0	c	0.12	1.42	13.18	16.28	74.60	1.24	1.82	3.59	2.83	4.55	8.83
10	1:1	2	d	0.17	1.40	10.17	12.50	81.50	0.96	1.45	2.57	1.74	3.73	7.27
11	1:1	5	a	0.39	1.38	7.92	10.75	94.50	0.86	0.92	2.07	2.16	2.85	6.25
12	1:1	8	b	0.52	1.36	6.67	9.33	98.20	0.64	0.93	1.98	1.69	2.60	4.75
13	2:1	0	d	0.10	1.25	16.83	19.58	45.90	0.82	1.24	2.40	1.52	3.35	5.18
14	2:1	2	c	0.13	1.22	11.92	15.80	73.60	0.49	0.46	1.01	0.59	1.09	1.56
15	2:1	5	b	0.15	1.20	10.58	13.08	87.65	0.30	0.50	0.65	0.45	0.80	1.36
16	2:1	8	a	0.22	1.18	7.17	10.42	91.60	0.21	0.29	0.44	0.35	0.49	0.92

Table 6. Range of grout properties under various influence factors and their sensitivity ranking to those factors.

Physical and Mechanical Property Parameters	Water–Cement Mass Ratio (A)	Content of Sodium Silicate (B)	Hydro-Chemical Type (Mining) (C)	Sensitivity Ranking
density/Kg.m ⁻³	0.36	0.08	0.01	A > B > C
viscosity/Pa.s	0.60	0.52	0.26	A > B > C
Initial setting time/h	4.27	7.02	0.98	B > A > C

Table 6. Cont.

Physical and Mechanical Property Parameters	Water–Cement Mass Ratio (A)	Content of Sodium Silicate (B)	Hydro-Chemical Type (Mining) (C)	Sensitivity Ranking
Final setting time/h	4.89	7.49	0.71	B > A > C
Stone rate/%	22.84	21.24	13.15	A > B > C
Flexural strength/MPa	3 d	1.82	0.66	A > B > C
	7 d	2.36	0.67	A > B > C
	28 d	3.37	1.70	A > B > C
Compressive strength/MPa	3 d	5.13	1.24	A > B > C
	7 d	8.18	2.11	A > B > C
	28 d	14.34	8.02	A > B > C

4. Grout Propagating Mechanism of Inclined Single Fracture in Horizontal Grouting Hole

Cement grout is widely used in current advanced regional grouting projects because of cost, environmental protection, grout performance and pumping technology. Due to the large volume of grout used in grouting projects, grout cement with a high water–cement ratio and good fluidity is generally used to ensure an optimal grout propagation length and a maximum grout coverage area. Grout viscosity is an important index of the fluidity of grout and has an important effect on the grout propagation length. However, the viscosity of grout with a water–cement ratio greater than 1.0 has a relatively small velocity vector change and can be regarded as a Newtonian fluid. The viscosity of grout with a water–cement ratio of less than 1.0 has time-varying characteristics [18]. According to Zhao [19], the water–cement ratio of cement grout used in advanced regional grouting projects is generally greater than 1.0, so that grout can be analyzed as a Newtonian fluid. This section will build and analyze the propagating mechanism of Newtonian fluid in a single inclined fracture of a horizontal borehole.

4.1. Basic Assumptions of Model Construction

The following derivation incorporates the following assumptions: (1) the grout propagation is continuous; (2) the grout is isotropic and incompressible and the bulk density and viscosity remain unchanged during the flow; (3) the inner wall of the grouting pipe meets no-slip boundary conditions; the upper and lower surfaces of the fracture are fully free of sliding boundary conditions; (4) that is, the grout flow velocity at the upper and lower surfaces is 0; (5) the width of the fracture is uniform; and (6) the grout propagation mode is complete displacement diffusion, without considering the mixing of water and grout at the grout and water interface.

4.2. Grout Propagating Model of an Inclined Single Fracture

Figure 2 is a schematic diagram of various forces of grout in an inclined parallel fracture of a horizontal grouting hole. According to the assumptions, the grout is subject to mass force, surface pressure and grout viscosity resistance in the flow process; the surface pressure includes grouting pressure and hydrostatic pressure. To facilitate the analysis, x - and y -axes were established along the parallel and vertical inclined fracture directions, respectively. The width of the fracture was $2h$, the intersection point of the horizontal grouting hole and the fracture was coordinate 0, the angle between the fracture and the horizontal hole was α and the hydrostatic pressure was p_0 .

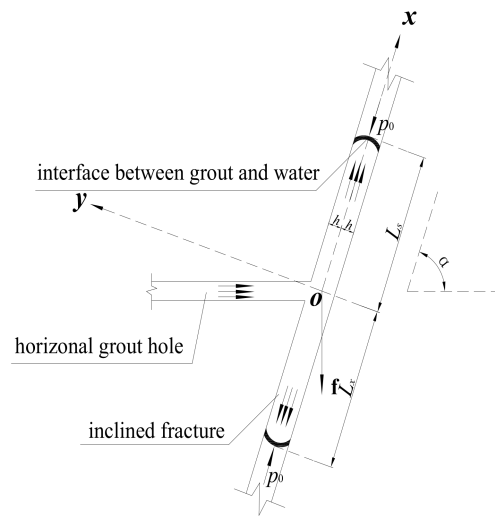


Figure 2. Grout force in a horizontal grouting hole inclined parallel fracture.

The early mathematician Euler constructed the mathematical equation of the motion of an inviscid fluid, and viscosity is a physical property of a fluid. Subsequently, Navier and Stokes added a viscosity term to the fluid motion equation and established the basic equation of viscous fluid mechanics. That equation describes the equilibrium relation of viscous fluid under the action of various forces. The continuity and constitutive equations comprise the basic equations of incompressible viscous flow [20]. When the viscosity is constant, that is, for Newtonian fluid, the Navier–Stokes vector equation can be simplified as

$$\frac{DV}{Dt} = \mathbf{f} - \frac{1}{\rho} \mathbf{grad} p + \nu \nabla^2 \mathbf{u} \tag{1}$$

where $\frac{DV}{Dt}$ is the acceleration of the grout mass micro-cluster under the action of force, \mathbf{f} is the unit mass force, the second term is the surface force generated by a pressure gradient and the third term is the friction force caused by grout viscosity.

Combined with the effect of the unit mass force in the grout movement, the unit mass force component in the x -axis direction is obtained by

$$f_x = \begin{cases} g \sin \alpha, & (x < 0) \\ -g \sin \alpha, & (x > 0) \end{cases} \tag{2}$$

First, the grout propagation in the fracture under the horizontal grouting hole (i.e., $x < 0$) is deduced and analyzed.

$\frac{DV}{Dt}$ is the partial differential component of the space vector of the fluid velocity (u, v, w) , so its component along the x direction is

$$\frac{\partial u}{\partial t} + u \frac{\partial u}{\partial x} + v \frac{\partial u}{\partial y} + w \frac{\partial u}{\partial z} \tag{3}$$

$\mathbf{grad} P$ is the partial differential component of surface pressure P in three directions in space and its component along the x direction is $\frac{\partial p}{\partial x}$.

$\nu \nabla^2 u^2$ is the component of viscous friction along the x direction and ν is the kinematic viscosity coefficient. Its relationship with viscosity μ is $\nu = \frac{\mu}{\rho}$: when the viscosity is constant, the component of viscous friction force in the x direction is

$$\frac{\mu}{\rho} \left(\frac{\partial^2 u}{\partial x^2} + \frac{\partial^2 u}{\partial y^2} + \frac{\partial^2 u}{\partial z^2} \right) \tag{4}$$

As shown in Equation (5), the scalar equation of the Navier–Stokes vector equation in the x direction can be obtained by substituting Equations (3) and (4) and the pressure gradient and unit mass force components into Equation (4):

$$\frac{\partial u}{\partial t} + u \frac{\partial u}{\partial x} + v \frac{\partial u}{\partial y} + w \frac{\partial u}{\partial z} = g \sin \alpha - \frac{1}{\rho} \frac{\partial p}{\partial x} + \frac{\mu}{\rho} \left(\frac{\partial^2 u}{\partial x^2} + \frac{\partial^2 u}{\partial y^2} + \frac{\partial^2 u}{\partial z^2} \right) \quad (5)$$

In addition, the continuity equation is a mass balance equation based on the law of conservation of mass:

$$\frac{\partial u}{\partial x} + \frac{\partial v}{\partial y} + \frac{\partial w}{\partial z} = 0 \quad (6)$$

Because the grout flows along the inclined fracture, according to the assumption that the grout flows only along the x direction and is infinitely extended in the z direction, the velocity change of the grout in the z direction is 0 and the velocity change outside the width in the y direction is 0. Combined with Equation (6), it is concluded that

$$\frac{\partial v}{\partial y} = 0, \frac{\partial w}{\partial z} = 0, \frac{\partial u}{\partial x} = 0 \quad (7)$$

Based on the assumption that the grout flow is steady, the following conclusion can be obtained:

$$\frac{\partial u}{\partial t} = 0$$

Thus, the Navier–Stokes Equation (5) in the x direction can be transformed into

$$g \sin \alpha - \frac{1}{\rho} \frac{\partial p}{\partial x} + \frac{\mu}{\rho} \frac{\partial^2 u}{\partial y^2} = 0 \quad (8)$$

Based on the assumption that the inner wall of the grouting hole is a slip-free boundary, the boundary condition can be obtained:

$$y = \pm h, u = 0 \quad (9)$$

Based on the boundary condition, the integral solution of Equation (8) is obtained:

$$u_x = \frac{1}{2\mu} \left(-\rho g \sin \alpha + \frac{\partial p}{\partial x} \right) (y^2 - h^2) \quad (10)$$

The average velocity of the slurry flow in the inclined fracture is obtained by

$$\bar{u}_x = -\frac{h^2}{3\mu} \left(-\rho g \sin \alpha + \frac{\partial p}{\partial x} \right) \quad (11)$$

We assume that the grouting pressure at the hole where the horizontal grouting hole intersects with the fracture is p_1 . After the grout enters the fracture from the grouting hole, the pressure decreases due to the resistance of hydrostatic pressure, the grout viscosity and the mass gravity and finally balances with the hydrostatic pressure, grout viscosity and mass gravity. Therefore, we assume that the front pressure of grout is p_0 ; that is to say, the hydrostatic pressure p_0 . When the grout propagation length along the fracture below the horizontal grouting hole reaches L_x , the boundary conditions are

$$\begin{cases} x = 0, p = p_1 \\ x = -L_x, p = p_0 \end{cases} \quad (12)$$

Then Equation (10) can be transformed into

$$\bar{u}_x = \frac{h^2}{3\mu} \left(\rho g \sin \alpha + \frac{p_1 - p_0}{L_x} \right) \quad (13)$$

We assumed that, after the horizontal grouting holes expose the fractures, the grout propagates around the fractures and then the circular shape of the grout–water interface front forms in the upper and lower fractures of the grouting hole. Therefore, the relation between the propagation length and the grouting quantity is obtained by the relation between the average propagation velocity and length. Then the relations among the grouting volume, the grout propagation length and the grouting pressure are obtained, which is the Newtonian grouting propagation model for cement grout in an inclined single fracture.

Take the fracture under the horizontal grouting hole as an example. Supposing that the radius of the grouting hole is r_0 , the crack opening is b and the diffusion distance of the slurry in the crack below the borehole is x within duration t , the grouting amount in the fracture below is obtained by

$$Q_x = \pi x \cdot b \cdot \bar{u}_x t \quad (14)$$

By substituting the average flow rate of grout in the fracture section below the horizontal grouting hole [Equation (10)] into the integral of both sides of Equation (14), we can get the following result:

$$p_x = \frac{12Q_x\mu}{\pi tb^3} \ln(-x) + \rho g \sin \alpha x + C \quad (15)$$

Based on the pressure at the orifice of the horizontal grouting, p_1 , we can get the following result:

$$p_x = p_1 + \frac{12Q_x\mu}{\pi b^3 t} \ln\left(-\frac{x}{r_0}\right) + \rho g \sin \alpha (x - r_0) \quad (16)$$

Based on the boundary condition (9), the following results are obtained:

$$Q_x = \frac{\pi tb^3}{12\mu} [p_0 + \rho g \sin \alpha (L_x + r_0) - p_1] \ln \frac{r_0}{L_x} \quad (17)$$

In the same way, the governing equations of the average velocity of the grout cross-section, grouting pressure and grouting quantity in the fracture above the horizontal grouting hole (when $x > 0$) are the following, respectively:

$$\bar{u}_s = \frac{h^2}{3\mu} \left(-\rho g \sin \alpha + \frac{p_1 - p_0}{L_s} \right) \quad (18)$$

$$p_s = p_1 - \frac{12Q_s\mu}{\pi b^3 t} \ln \frac{x}{r_0} - \rho g \sin \alpha (x - r_0) \quad (19)$$

$$Q_s = \frac{\pi tb^3}{12\mu} [(p_1 - p_0) - \rho g \sin \alpha (L_s - r_0)] \ln \frac{r_0}{L_s} \quad (20)$$

The grout flow in the fracture section can be obtained based on the average velocity (Equation 13)) and flow calculation equation of grout propagation in the inclined single fracture. For the fracture ($x < 0$) under the horizontal grouting hole, Equation (10) is introduced into Equation (14) and the cross-section flow in the fracture under the horizontal grouting hole is obtained by dividing the grouting amount by the duration:

$$q_x = \frac{\pi b^3}{12\mu} (p_1 - p_0 + \rho g \sin \alpha L_x) \quad (21)$$

The amount of grout injected into the fracture in a unit of time should be equal to the amount of slurry required to increase the diffusion radius r in this period:

$$\int_0^t q_x dt = \int_{r_0}^{L_x} \pi b L_x dL \quad (22)$$

By introducing Equation (21) into Equation (22), we can get the following results:

$$t = \frac{6\mu(L_x^2 - r_0^2)}{b^2[(p_1 - p_0) + \rho g L_x \sin \alpha]} \quad (23)$$

In the same way, the grouting duration of the cracks above the horizontal grouting hole (when $x > 0$) is obtained by

$$t = \frac{6\mu(L_s^2 - r_0^2)}{b^2[(p_1 - p_0) - \rho g L_s \sin \alpha]} \quad (24)$$

The control equation of grout diffusion distance without a grouting amount can be obtained by transforming the control equation of grouting duration:

$$6\mu L^2 \pm \rho g \sin \alpha b^2 t L - (p_1 - p_0) b^2 t - 6\mu r_0^2 = 0 \quad (25)$$

(Take “+” as the crack above the horizontal grouting hole and “−” as the crack below the horizontal grouting hole.)

5. Grouting Control Method of Horizontal Grouting Hole at the Top of Middle Ordovician Limestone

5.1. Analysis of Influencing Factors of Grout Propagation Length in a Single Fracture

Based on the grout propagation length in an inclined single fracture, there are many controlled factors for grout propagation length in a fractured rock mass, such as the fracture width, angle between fracture and grouting hole, grouting pressure, grouting duration, grout viscosity, grout specific weight and grouting volume. Among the rest, grouting pressure, grouting duration, grout performance and grouting volume are controllable. In contrast, the fracture width, the angle between the fracture and the grouting hole and the hydrostatic pressure are properties inherent to the injected rock. Therefore, in engineering practice, controlling the grout propagation length is achieved by adjusting the controllable grouting parameters such as grouting pressure, grouting duration, grout performance and grout amount to master the objective attribute parameters of the injected rock. To quantitatively analyze the influence characteristics of grout propagation length on the controllable grouting parameters and the inherent parameters of injected rock, we used MATLAB software to analyze the variation characteristics of grout propagation length under various influence factors by using a method that controlled the variables.

Based on Equation (25), the value of grout propagation length L with grouting duration t under various grout viscosities μ , grouting pressures p_1 , angle between fracture and grouting hole α , crack opening b and hydrostatic pressure p_0 were calculated and the variation characteristics were analyzed. Among them, the radius of the horizontal grouting hole r_0 was 0.076 m, the hydrostatic pressure p_0 was 10^7 Pa, the duration range was 0 to 6000 s and the gravity acceleration g was $9.8 \text{ m}\cdot\text{s}^{-2}$.

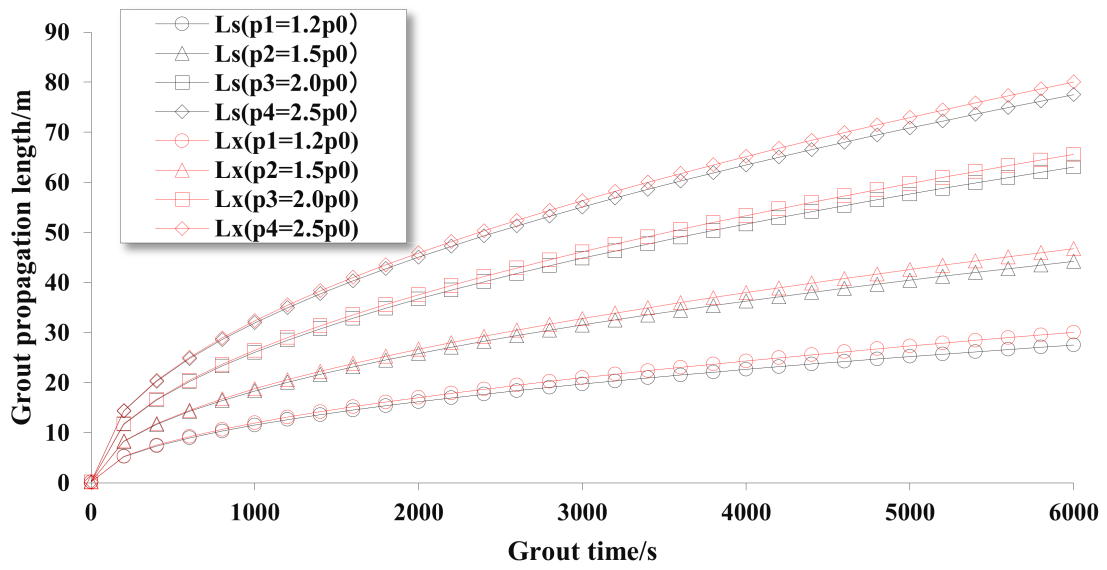
As shown in Table 7, the grout pressure, fracture width, angle and water–cement ratio were the factors that were changed by fixing other parameters. So the variation value of grout propagation length with duration under the changed factors was calculated. We also obtained the variation characteristics of grout propagation length under the changed factors.

Table 7. Calculation parameters of grout propagation length under various factors. (a) Grout pressure. (b) Fracture width. (c) Angle between fracture and horizontal hole. (d) Water–cement ratio.

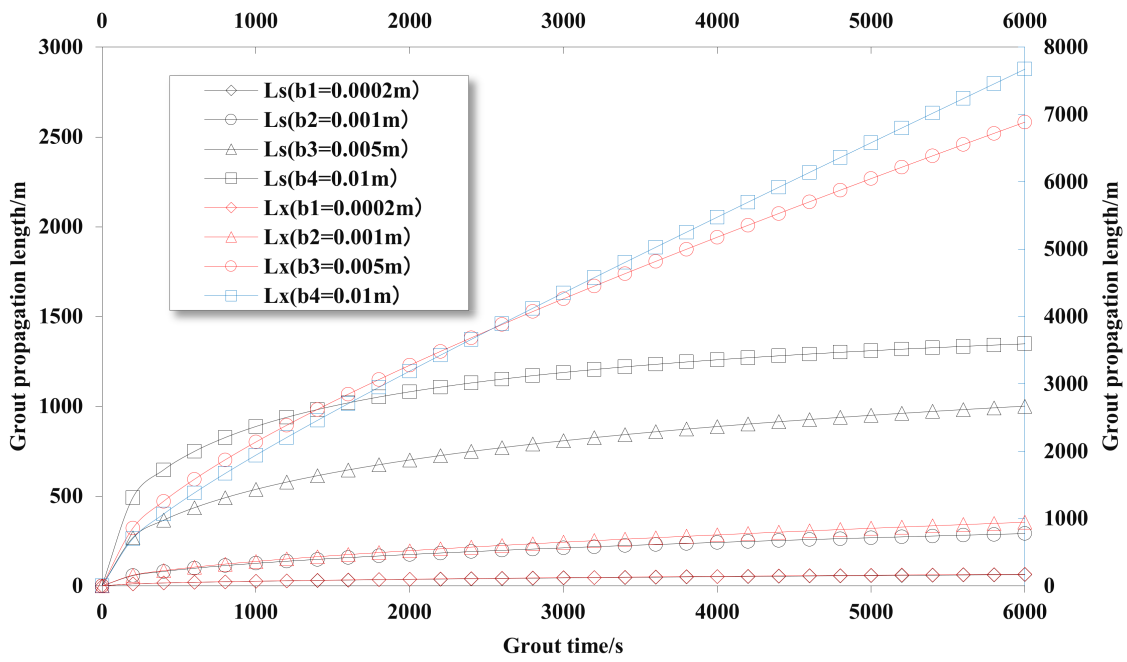
Number	Level	Water–Cement Ratio	Viscosity/Pa·s	Density/Kg.m ⁻³	Width of Fracture/m	Angle/°	Grout Pressure/Pa
1	grout pressure	2:1	0.0967	1248	0.0002	30	1.2 × 10 ⁷ 1.5 × 10 ⁷ 2.0 × 10 ⁷ 2.5 × 10 ⁷
2	width of fracture	2:1	0.0967	1248	0.0002 0.001 0.005 0.01	30	2 × 10 ⁷
3	angle	2:1	0.0967	1248	0.0002	0 30 60 90	2 × 10 ⁷
4	water–cement ratio	3:1 2:1 1:1	1160 1248 1424	0.0742 0.0967 0.1198	0.0002	30	2 × 10 ⁷

Figure 3 shows that, under various influencing factors, the grout propagation length increases over time. The grout propagation length also increases with an increase in grout pressure, fracture width and the water–cement ratio. In addition, with an increase in duration, the gap of the grout propagation length increases gradually with an increase in any of the above three factors. For example, the grout propagation length increases with an increase in the grout pressure and this trend becomes more and more obvious over time (Figure 3a). This indicates that the influence of grouting pressure on grout propagation length has an obvious duration effect. Similar to the influence of grouting pressure on grout propagation length are the fracture width and the ratio of water to cement (Figure 3b,c). However, under the influence of the water–cement ratio this feature is not obvious. Under the influence of the fracture width, the grout propagation length from an open fracture (0.001 m) to a moderately tensioned fracture (0.005 m) increases most and that gap gradually increases over time. By comparing the grout propagation lengths in fractures of various sizes, it can be seen that, under a higher grouting pressure (two times the hydrostatic pressure), the increase in propagation length in a closed fracture (0.0002 m) or a micro-tension fracture is minor.

Furthermore, for the same duration and the same value of the influencing factor, the grout propagation length under a horizontal grouting hole was larger than that above the horizontal grouting hole. This is because, in the upper fracture, gravity resisted the grout movement, while in the lower fracture gravity played a dynamic role. Moreover, this feature was most obvious under the influence of the fracture width. Comparing the grout propagation lengths in the fractures above and below the horizontal grouting hole, the length in the lower fracture was larger than that in the upper fracture at the scales of a closed fracture, a micro-tension fracture and a medium-tension fracture. The differences increased with an increase in fracture width. However, in the wide tensile fracture, the grout propagation length in the upper fracture was larger than that in the lower fracture within 1500 s. However, after 1500 s, the grout propagation length in the lower fracture was gradually greater than that in the upper fracture and the difference was doubled. This phenomenon was consistent with the findings of Li and Wang (2014) regarding the grout propagation length in the upper and lower fractures of a grouting hole obtained from a grout propagation model test done with an inclined plate crack with a gap width of 3 mm.

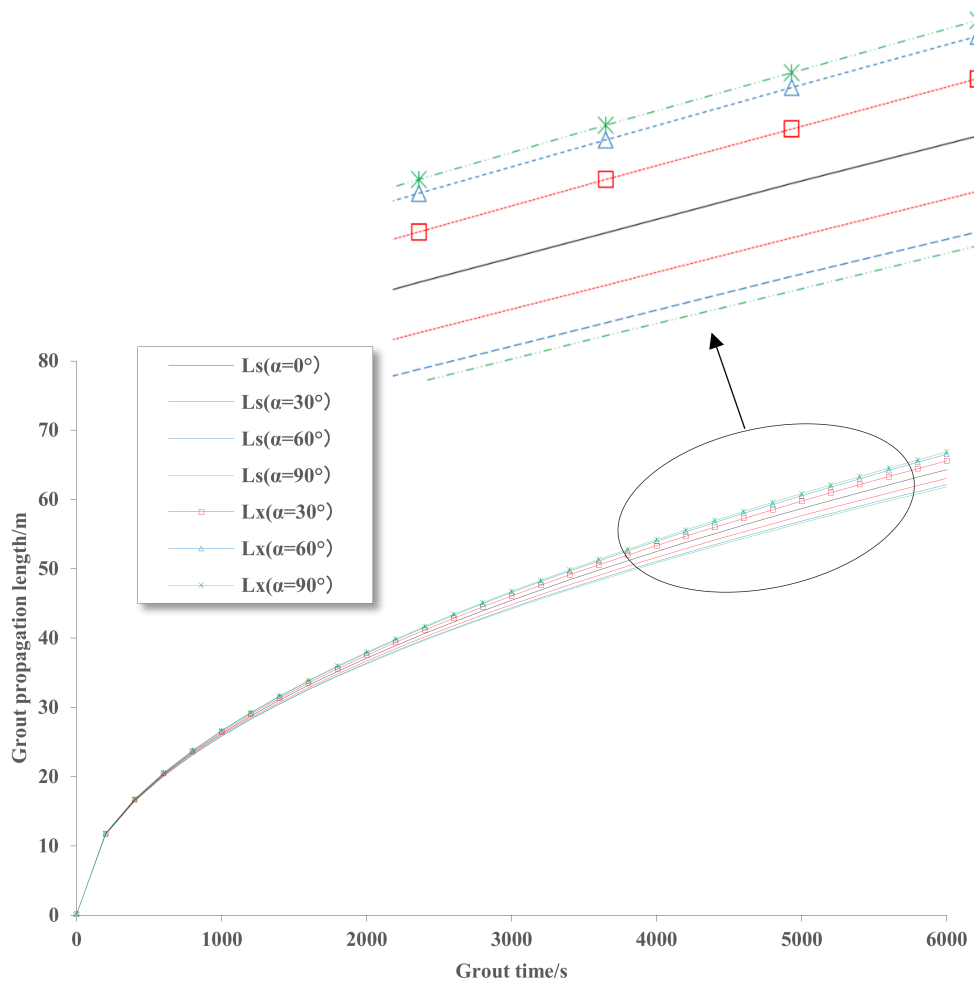


(a)

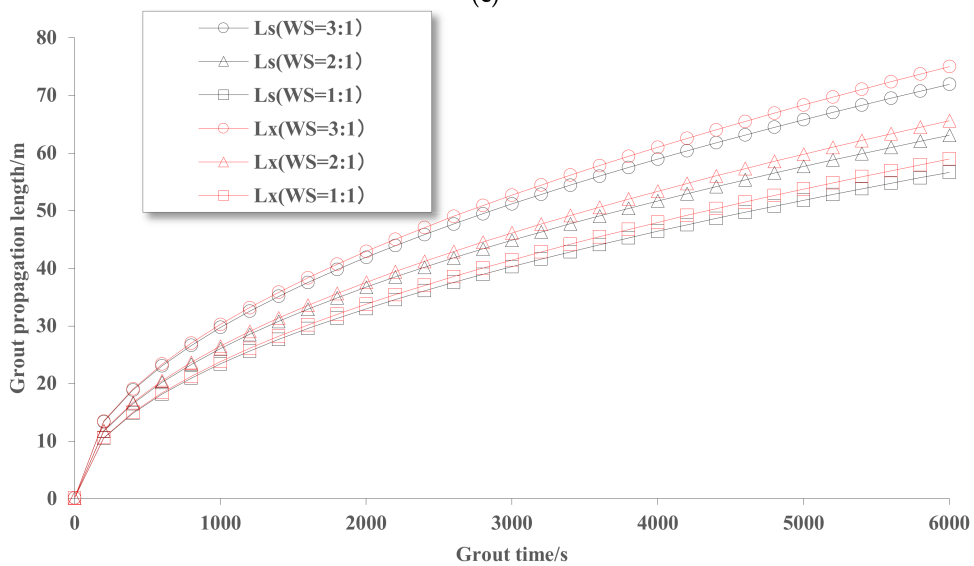


(b)

Figure 3. Cont.



(c)



(d)

Figure 3. Variation curve of grout propagation length with duration under various influencing factors. (a) Grout pressure, (b) width of fracture, (c) angle between fracture and horizontal hole, (d) water-cement ratio.

However, the influence of different angles between the fracture and the horizontal grouting hole showed some characteristics different from those of the above factors (Figure 3d). For the influence of the angle between the fracture and the horizontal grouting hole, with an increase in grouting duration, the grout propagation length increased, but the tendency was not obvious relative to that of other factors. In addition, the grout propagation length for different angles under the horizontal grouting hole was greater than that above the horizontal grouting hole. Based on this, the influence of different angles between fracture and the horizontal grouting hole on the grouting propagation length appeared relatively minor.

5.2. Numerical Calculation of Grout Propagation Based on Orthogonal Test

Following the $L_9(3^4)$ orthogonal table design method, we designed three levels by considering the water–cement ratio, grouting pressure, fracture width and angle between fractures and borehole. Therefore, there were nine calculation conditions. We used COMSOL numerical simulation software to analyze and calculate the influence of the grout propagation length of a single fracture in a horizontal grouting hole. The selected factors and levels are shown in Table 8 and the nine numerical simulation conditions are shown in Table 9. We obtained the grout propagation pattern and grouting pressure distribution results under various working conditions for 1 h according to the calculations, as shown in Figures 4–12.

Table 8. Numerical simulation factors and levels.

Factors	Levels		
	1	2	3
water–cement ratio	1:1	2:1	3:1
grouting pressure/MPa	15	20	25
width of fracture/mm	1	5	10
angle of fracture/°	30	60	90

Table 9. Numerical simulation working conditions.

Number	Water–Cement Ratio	Grouting Pressure/MPa	Width of Fracture/mm	Angle of Fracture/°
1	1:1	15	1	30
2	1:1	20	5	60
3	1:1	25	10	90
4	2:1	15	5	90
5	2:1	20	10	30
6	2:1	25	1	60
7	3:1	15	10	60
8	3:1	20	1	90
9	3:1	25	5	30

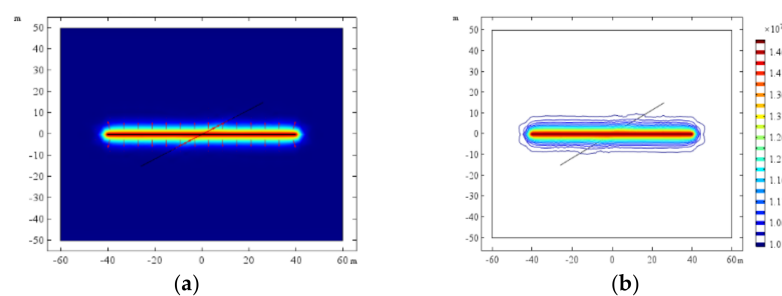


Figure 4. Case 1 calculation result. (a) Grout propagation pattern. (b) Distribution of grout propagation pressure field.

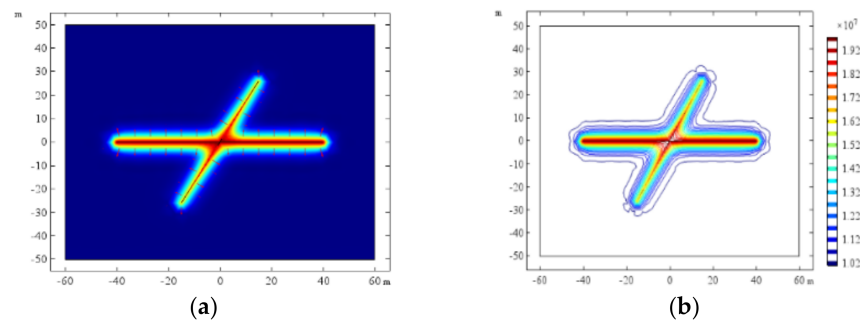


Figure 5. Case 2 calculation result. (a) Grout propagation pattern. (b) Distribution of grout propagation pressure field.

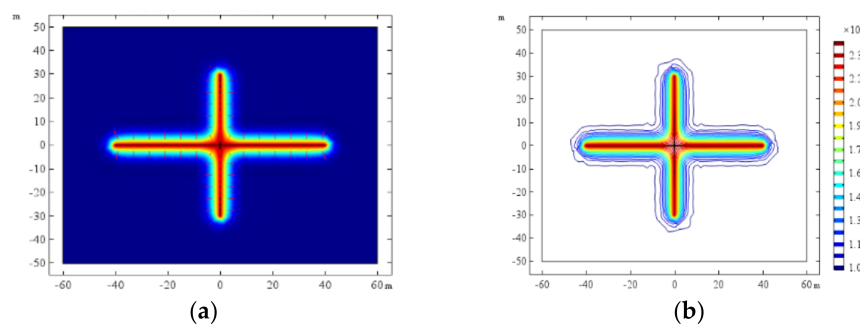


Figure 6. Case 3 calculation result. (a) Grout propagation pattern. (b) Distribution of grout propagation pressure field.

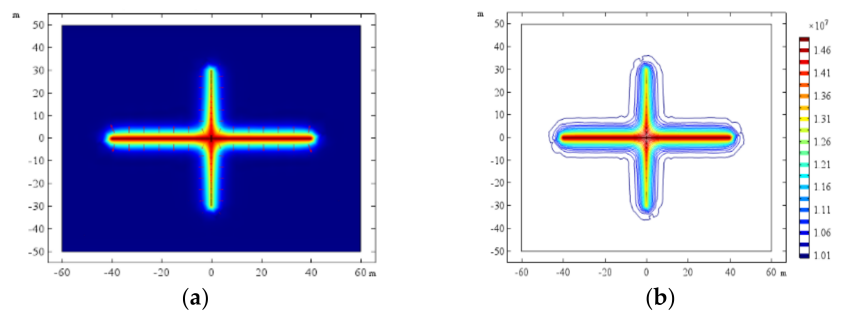


Figure 7. Case 4 calculation result. (a) Grout propagation pattern. (b) Distribution of grout propagation pressure field.

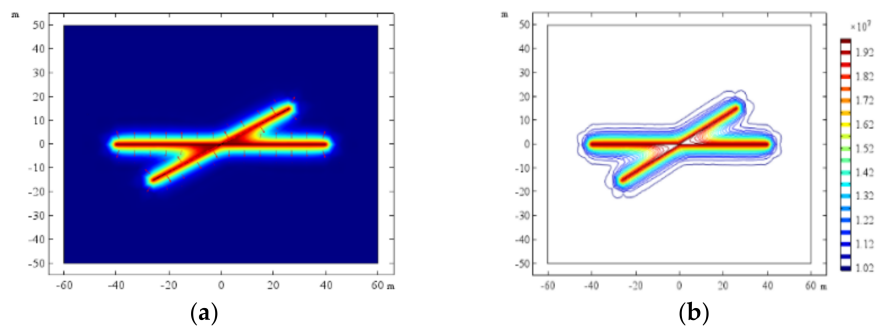


Figure 8. Case 5 calculation result. (a) Grout propagation pattern. (b) Distribution of grout propagation pressure field.

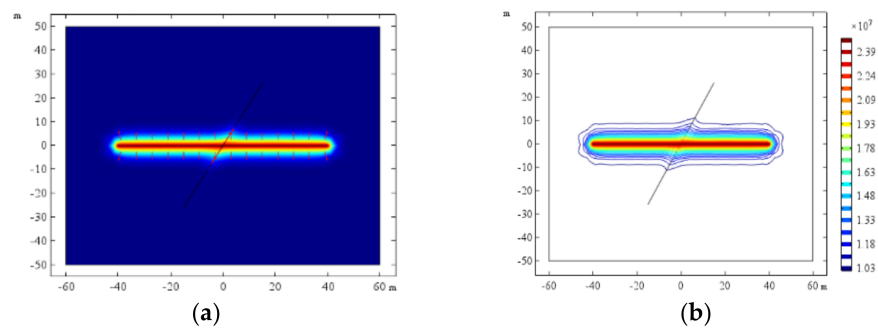


Figure 9. Case 6 calculation result. (a) Grout propagation pattern. (b) Distribution of grout propagation pressure field.

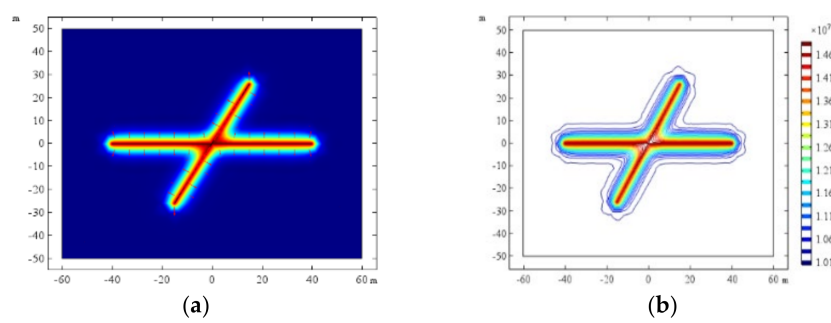


Figure 10. Case 7 calculation result. (a) Grout propagation pattern. (b) Distribution of grout propagation pressure field.

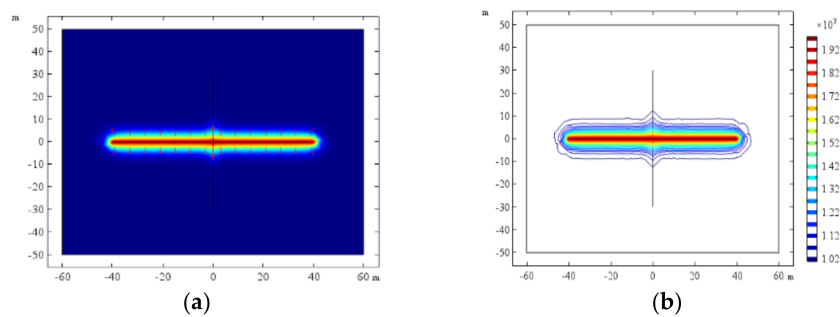


Figure 11. Case 8 calculation result. (a) Grout propagation pattern. (b) Distribution of grout propagation pressure field.

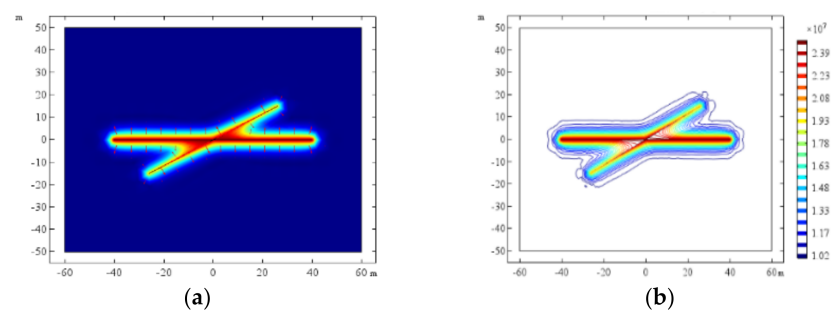


Figure 12. Case 9 calculation result. (a) Grout propagation pattern. (b) Distribution of grout propagation pressure field.

Figures 4–12 show that, with the increase in grouting duration, the grout propagation length increased gradually. Due to the influence of hydrostatic pressure, grout viscosity

and self-gravity, the force of the grout movement was gradually lost and the increase in its propagation length decreased with the increase in duration. Therefore, when the grout propagated to a certain length, the grouting pressure, the aquifer pressure, the grout viscosity resistance and other factors reached a dynamic balance and the grout propagation length tended to be stable. However, the grouting pressure was the greatest at the orifice of the horizontal grouting hole and the pressure gradient gradually decreased with the increase in the distance from the orifice. In addition, the grout had an obvious compression effect on the rock mass under pressure, but that effect decreased with the increase in the distance from the inner wall of the grouting hole, so the pressure field distribution law gradually decreased. With the increase in grouting duration, the grout propagation length increased, the grout and the resistance in the fracture reached equilibrium and the grout propagation distance did not increase in the ideal state.

The grout propagation length was obtained by analyzing the equilibrium state of grout and resistance under the working conditions (Table 10). We obtained the range value of each factor in accordance with the principle of the orthogonal test. The larger the range value, the greater the influence of the factor on the results. Therefore, it can be seen from the test results that the range of factor C was the largest; that is, the width of the fracture had the most significant effect on the grout propagation length. According to the range of each factor, the sequence of the sensitivity of each factor to the test results from large to small was fracture width, fracture angle, water–cement ratio and grouting pressure. The fracture width and angle were the inherent properties of a rock mass. Therefore, it is of great significance to master the development degree of fractures in an aquifer for an early grouting process design. According to the above calculation results, the sensitivity of the influence of the water–cement ratio on the grout propagation length is greater than that of the grouting pressure. Therefore, in an actual grouting process the water–cement ratio should be given priority.

Table 10. Range analysis of numerical simulation results.

	Factor				Grout Propagation Length/m
	A	B	C	D	
1	1:1	15	1	30	46
2	1:1	20	5	60	41.57
3	1:1	25	10	90	48
4	2:1	15	5	90	43
5	2:1	20	10	30	56
6	2:1	25	1	60	27.71
7	3:1	15	10	60	42.73
8	3:1	20	1	90	24.5
9	3:1	25	5	30	53
mean value 1	45.19	43.91	32.74	51.67	/
mean value 2	42.24	40.69	45.86	37.34	/
mean value 3	40.08	42.90	48.91	38.50	/
xmax-xmin	5.11	3.22	16.17	14.33	/

5.3. Control Method of Grout Propagation Length

The grouting reinforcement region is certain, but the fracture network in the aquifer may be infinitely extended. Consequently, in advanced regional grouting projects, grout propagation in the reinforcement region should be controlled. In a coal mine floor advanced regional grouting project, many factors affect grout propagation, such as the pore development characteristics of the grouting target strata, grouting materials, water–cement ratio, grouting pressure and grouting duration. How to control these factors is the key to determining the effect of the project. To achieve a good grouting effect with grout propagation control, the key is to devise an effective grouting end standard. Among the above factors, the water–cement ratio of the grout, the grouting pressure and the grouting duration are the controllable factors in engineering practice. The grouting end standard depends on the

conditions of the grouting target strata, the spacing between horizontal grouting holes and grouting equipment and other factors. Therefore, the control of grout propagation should be based first on a reasonable spacing between horizontal holes according to the conditions of the grouting target strata, grouting equipment, grouting pressure and grouting duration. Then, the grouting end standard that consists of grouting end pressure and stabilizing duration corresponding to the spacing between horizontal grouting holes should be determined. By analyzing the characteristic curve of the grout propagation length in an inclined single fracture under various conditions, the grout propagation length can be obtained for various water–cement ratios, conditions of the grouting target strata and grouting pressures. The spacing between horizontal holes to meet the working capacity of the grouting equipment can be obtained by restricting the rated working capacity of the equipment. To determine the grout propagation overlap and coverage between horizontal holes, after the distance between horizontal holes is determined, the grouting end pressure and duration standard can be found by regulating the water–cement ratio, grouting pressure and grouting duration.

The basis for regulating the ratio of grout to water to cement, grouting pressure and grouting duration is the influence of the grout propagation length mentioned above in the characteristics and sensitivity ranking principle. Specifically, based on the analysis of the characteristics of grout propagation for advanced regional grouting projects, using lower grouting pressure in the early stage of grouting can reach the established grout propagation range by increasing grouting duration. In addition, the grouting duration should not be too long in the stage of pressure grouting. Considering that the number of closed fractures or micro open fractures is in the majority, high-pressure split grouting should be used after the short-term booster grouting to achieve expansion and filling of closed fractures or micro open fractures. The grout propagation length of medium- or wide-tension fractures (0.01 m) can reach more than 1000 m or even greater over time. Therefore, mining should be carried out early in the grouting process when low-pressure grouting is used to prevent the grout from exceeding the designed propagation range. In addition, for the low-pressure grouting stage, when the duration is long, the water–cement ratio of the grout should be reduced over time to limit the continuous increase in grout propagation length over time. Although the propagation length of grout with various water–cement ratios in fractures below the horizontal grouting hole is greater than that in fractures above and expands with time, the difference is not obvious for fractures of 0.0002 m.

The specific method route is shown in Figure 13.

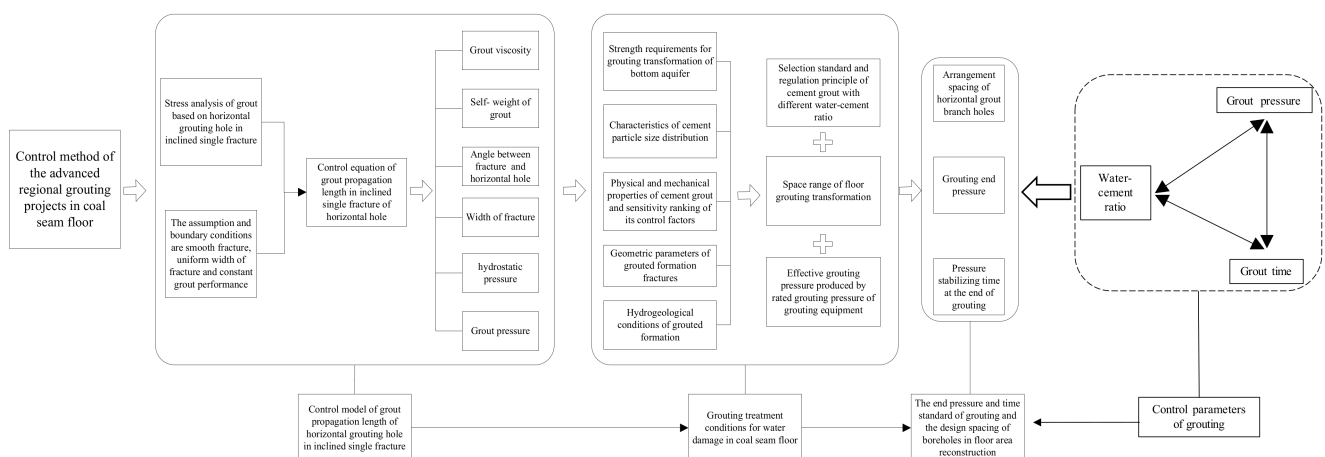


Figure 13. Technical route of grout propagation control method for advanced regional grouting projects in coal floors.

6. Engineering Application

The production capacity of one of the mines in the Hanxing mining area is 3 million tons per year. Seam No. 2 of the lower part of the Shanxi formation of the Permian system

is the one that is mainly mined. The average thickness of the coal seam is 3.17 m and the coal seam stope is more than 950 m from the surface. The coal seam floor contains Yeqing, Shanfuqing, Daqing and Ordovician limestones and multiple other aquifers, among which the MOL is the main aquifer threatening the safety of mine production. The aquifer is 135 to 150 m away from the bottom of the No. 2 coal seam, for an average of 145 m. It is the basement of the coal measure strata, with a thickness of approximately 600 m. It is a karst-fissure, karst-cave aquifer with a strong water yield. The unit water inflow is 1.258 to 6.438 L/s.m and the water level elevation is approximately +130 m.

According to the Hebei Province Coal Mine Water Prevention and Control Management Measures, the “Hanxing area mining depth greater than 800 m hydrogeological type of extremely complex mine should adopt the surface advanced regional grouting project.” Therefore, the mine adopts that grouting reinforcement technology required for advanced regional grouting on the top of the MOL aquifer, to block the karst fractures and hidden water passages, barricade the groundwater and achieve safe mining of the coal seam. This study selected the advanced regional treatment of the fourth mining area of the mine as a case study. The target layer of the fourth mining area was the top of the MOL aquifer, the ground elevation of the grouting hole was +150.3 m, the water level of the Ordovician limestone aquifer was +132 M and the lowest elevation of the mining area was −1060 m.

Due to the development of karst fissures and caves in the MOL aquifer in the mining area, the grouting process was generally pressureless grouting and booster grouting. To ensure the grouting effect, parameters such as spacing between boreholes, grouting reinforcement range and grouting pressure were analyzed according to the grouting end parameters to guide the grouting design and engineering practice. Therefore, based on the relevant working condition parameters of the No. 4 mining area, we calculated the grouting end parameters by Equation (25). According to the analysis, the hydrostatic pressure of the MOL aquifer was 11.92 mPa. To ensure the grouting effect, the width of the fracture was 0.0002 m. In addition, because the water–cement ratio of grout is usually controlled at 1:1 to 3:1, the author used cement grout with a water–cement ratio of 1:1 for calculation. The grouting pressures were 1.5 times, 2.0 times and 2.5 times the hydrostatic pressure. In addition, to obtain the grout propagation range, the angle between fractures and horizontal grouting holes was 90 degrees. The calculation results are shown in Figure 14.

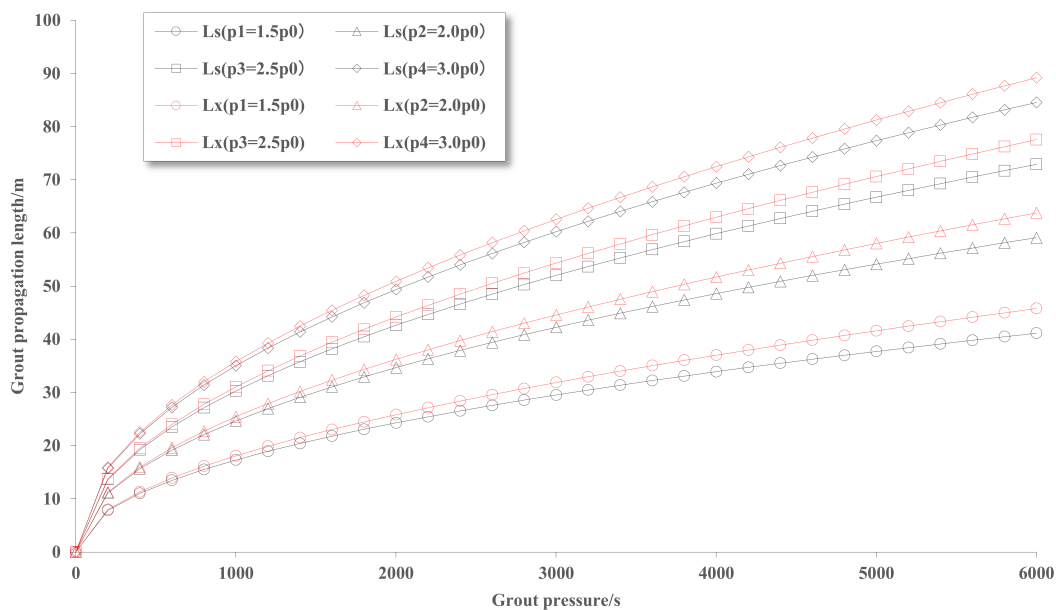


Figure 14. Calculation curve of slurry diffusion distance on top of Middle Ordovician limestone in No. 4 mining area.

Because of the rated grouting pressure of the grouting pump and the pressure tolerance of the grouting pipeline, the stability duration of the final pressure was generally controlled in the range of 30 to 35 min, as shown in Figure 14. When the grouting duration was 30 min, with a change in grouting pressure the grout propagation length was 23.75 to 48.17 m in the upper fracture and 25.14 to 49.57 m in the lower fracture. In addition, when 1.5 times the hydrostatic pressure was used for grouting, the spacing of the horizontal branch holes was not less than 47.5 m and the distance between horizontal branch holes and the interface of the Ordovician limestone top was not more than 23.75 m. Therefore, considering the grouting effect and construction technology, the final grouting pressure was designed to be no less than two times the aquifer hydrostatic pressure and the ratio of grout to water to cement was controlled at 3:1 to 1:1. The pressure stabilizing duration was more than 30 min, the spacing of the horizontal branch holes was 50 to 60 m and the drilling horizon was 30 to 60 m below the top surface of the Ordovician limestone.

Therefore, according to the design scope of the No. 4 mining area, six main holes and 24 Ordovician limestone horizontal branch holes were designed and constructed for the No. 1 hole. After drilling to 30 to 60 m below the top surface of the Ordovician limestone, directional drilling along the horizontal bedding of this layer was adopted and a “belt” and “feather” uniform hole distribution mode was adopted (Figure 15).

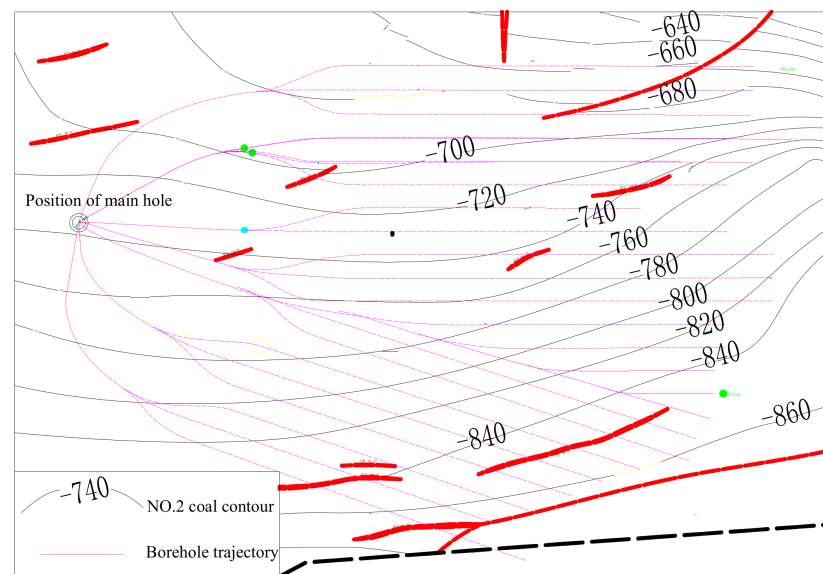


Figure 15. Design of main hole and Middle Ordovician limestone horizontal branch hole in the No. 4 mining area.

By analyzing the natural gamma value data of the 7 main holes and 24 horizontal branch holes constructed, we determined that the gamma value of the No. 2 coal in the mine was 15 to 35 API, the value of the mudstone was 100 API, the value of the eighth segment of the MOL was 10 to 20 API and the value of the seventh segment was 3 to 10 API. Note that the natural gamma-ray values of the coal seams, the aquifers and the MOL were different. This was the basis to distinguish the marker layer. Therefore, the construction horizon of the horizontal branch holes was controllable and accurate. Based on the leakage situation of a single horizontal branch hole, the belt or feather type hole layout was adopted and the leakage point area was densely drilled. During the construction, we ensured that the distance between the branch hole track and the original leakage point was not more than 55 m, reasonably arranged the construction sequence of the branch hole and verified the grouting effect by using adjacent boreholes. After the grouting treatment and subsequent cleaning, drilling and verification of the branch hole construction, no leakage was found near the original leakage point, indicating that the grouting plugging was effective. It shows that the design of grouting parameters such as drilling spacing and

grouting pressure was reasonable, the karst-fissure development section at the top of the MOL aquifer in the treatment area had been effectively reinforced by grouting and the purpose of aquifer transformation had been achieved.

7. Discussion

- (1) In the numerical calculation, there was no marked difference in the grout propagation length between the upper and lower fractures of the horizontal grouting holes under various working conditions. The main reason is that the grout propagation length was always in a small range. Relative to the previous theoretical analysis, the grout propagation lengths in the upper and lower fractures of the horizontal grouting holes differed only slightly, unless the grout propagation length was hundreds of meters or more. The phenomenon of a large difference in the range of the upper kilometer was consistent.
- (2) Under the condition of a wide-tension-fracture opening (0.01 m), there was a large gap between the numerical calculation results and the theoretical calculation results. The main reason was that the porosity of the rock mass was set in the numerical calculation and the fracture was filled with only water in the theoretical calculation. However, the spatial and temporal distribution characteristics of various factors on the grout propagation length could be accurately given by the numerical simulation calculation. The influence factors of distance had a good qualitative analysis effect.

8. Conclusions

- (1) Based on the factors of the grouting pressure, angle between crack and grouting hole, hydrostatic pressure, grouting volume, grout viscosity, fracture width, grout gravity and grouting duration, we established a mathematical model of Newtonian fluid slurry diffusion distance in the upper and lower cracks of horizontal grouting holes.
- (2) As determined by theoretical analysis, the slurry in an inclined single fracture of a horizontal grouting hole increases with an increase in grouting duration under various water–solid ratios, grouting pressure, crack opening and angle between crack and grouting hole and the increase rate decreases over time. However, the slurry diffusion distance in the fracture above the horizontal grouting hole is larger than that in the lower fracture when the grout propagation length is hundreds of meters or more and the difference increases multiple times under the wide fracture scale.
- (3) Based on the orthogonal design and numerical calculations, we obtained a sequence of the sensitivity of the factors affecting the diffusion distance of Newtonian grout in an inclined fracture of a horizontal grouting hole: from higher to lower, they were crack opening, fracture inclination angle, water–solid ratio and grouting pressure.
- (4) Based on the control equation of the grout diffusion distance of an inclined fracture in a horizontal grouting hole and grouting parameters for a mine in the fourth mining area, the horizontal spacing of branch holes was not more than 65.90 m and the interface distance between the branch holes and the Ordovician limestone roof was not more than 32.95 m, which is close to the engineering practice parameters.

Author Contributions: Conceptualization and Writing—original draft, Z.L.; Writing—review & editing, S.D.; Data curation, H.W.; Software, H.S. All authors have read and agreed to the published version of the manuscript.

Funding: This study was sponsored by the National Natural Science Foundation of China (Grant No.52104240) and Natural Science Basic Research Program of Shaanxi Province (No.2022JQ-320). The authors are grateful for their support.

Data Availability Statement: Not applicable.

Conflicts of Interest: The authors declare no conflict of interest.

References

1. Liu, S.; Fei, Y.; Xu, Y.; Huang, L.; Guo, W. Full-floor Grouting Reinforcement for Working Faces with Large Mining Heights and High Water Pressure: A Case Study in China. *Mine Water Environ.* **2020**, *39*, 268–279. [[CrossRef](#)]
2. Yin, S.; Zhang, J.; Liu, D. A study of mine water inrushes by measurements of in situ stress and rock failures. *Nat. Hazards* **2015**, *79*, 1961–1979. [[CrossRef](#)]
3. Zhang, W.J.; Li, S.C.; Wei, J.C.; Zhang, Q.S.; Liu, R.T.; Li, Z.P.; Sun, Z.Z. Relative Impermeability of the Ordovician Top and Risk Assessment of Water Inrush from Coal Floor in Baode Coalfield. *Adv. Mater. Res.* **2013**, *671*, 85–89. [[CrossRef](#)]
4. Qiu, M.; Huang, F.; Wang, J.; Shi, L.; Qu, X.; Liu, T. Characteristics of vertical karst development and grouting reinforcement engineering practice of the Ordovician top in the Feicheng coalfield, China. *Carbonate Evaporite* **2020**, *35*, 78. [[CrossRef](#)]
5. Yin, S.; Han, Y.; Zhang, Y.; Zhang, J. Depletion control and analysis for groundwater protection and sustainability in the Xingtai region of China. *Environ. Earth Sci.* **2016**, *75*, 1246. [[CrossRef](#)]
6. Yu, X.; Pei, F.; Han, J.; Gao, W.; Wang, X. Ordovician limestone karst development law in Feicheng coal field. *Environ. Earth Sci.* **2018**, *77*, 781. [[CrossRef](#)]
7. Hässler, L.; Håkansson, U.; Stille, H. Computer-simulated flow of grouts in jointed rock. *Tunn. Undergr. Space Technol.* **1992**, *7*, 441–446. [[CrossRef](#)]
8. El Tani, M. Grouting Rock Fractures with Cement Grout. *Rock Mech. Rock Eng.* **2012**, *45*, 547–561. [[CrossRef](#)]
9. Gustafson, G.; Claesson, J.; Fransson, A. Steering Parameters for Rock Grouting. *J. Appl. Math.* **2013**, *2013*, 269594. [[CrossRef](#)]
10. Li, S.; Han, W.; Zhang, Q.; Liu, R.; Weng, X. Research on time-dependent behavior of viscosity of fast curing grouts in underground construction grouting. *Chin. J. Rock Mech. Eng.* **2013**, *32*, 1–7.
11. Zhang, Q.; Zhang, L.; Zhang, X.; Liu, R.; Zhu, M.; Zheng, D. Grouting diffusion in a horizontal crack considering temporal and spatial variation of viscosity. *Chin. J. Rock Mech. Eng.* **2015**, *34*, 1198–1210.
12. Zou, L.; Hakansson, U.; Cvetkovic, V. Yield-power-law fluid propagation in water-saturated fracture networks with application to rock grouting. *Tunn. Undergr. Space Technol.* **2020**, *95*, 103170. [[CrossRef](#)]
13. Zou, L.; Hakansson, U.; Cvetkovic, V. Radial propagation of yield-power-law grouts into water-saturated homogeneous fractures. *Int. J. Rock Mech. Min.* **2020**, *130*, 104308. [[CrossRef](#)]
14. Zhao, Z.H.; Zhou, D. Mechanical properties and failure modes of rock samples with grout-infilled flaws: A particle mechanics modeling. *J. Nat. Gas Sci. Eng.* **2016**, *34*, 702–715. [[CrossRef](#)]
15. Hu, Y.; Liu, W.; Shen, Z.; Gao, K.; Liang, D.; Cheng, S. Diffusion mechanism and sensitivity analysis of slurry while grouting in fractured aquifer with horizontal injection hole. *Carbonate Evaporite* **2020**, *35*, 49. [[CrossRef](#)]
16. Nan, S. Technical feasibility of grouting reform for upper part of Ordovician limestone in Xingtai and Handan coal mining areas. *Coal Geol. Explor.* **2010**, *38*, 37–40. [[CrossRef](#)]
17. Li, T.; Gao, Y.; Chen, W. Characteristics of deep Ordovician limestone water and its concentrated application in Ordovician limestone water disaster prevention. *Mtan Xuebao/J. China Coal Soc.* **2018**, *43*, 262–268.
18. Pan, W.Y. Distribution regularities of the limestone and development of karst in North-China type coal fields. *J. China Coal Soc.* **1982**, *3*, 48–56.
19. Zhao, Q.B. Ordovician limestone karst water disaster regional advanced governance technology study and application. *J. China Coal Soc.* **2014**, *39*, 1112–1117.
20. Brebbia, C.A.; Connor, J.J. Boundary element formulation for viscous compressible flow. In *Viscous Flow Applications*; Springer: Berlin/Heidelberg, Germany, 1989; pp. 10–31.